High-resolution Climate Projections

over Minnesota for the 21st Century

Stefan Liess[1], Tracy E. Twine[1], Peter K. Snyder[1], William D. Hutchison[2], Gabriel Konar-Steenberg[1], Bonnie L. Keeler[3], Kate A. Brauman[4]

[1]Department of Soil, Water, and Climate [2]Department of Entomology [3]Humphrey School of Public Affairs [4]Institute on the Environment - University of Minnesota

Corresponding author address: Stefan Liess, Department of Soil, Water, and Climate, University of Minnesota, 1991 Upper Buford Circle, St. Paul, MN 55108, USA
Phone: (612) 624-0786, Fax: (612) 625-2208, Email: liess@umn.edu

Key Points:

- Over northern and central Minnesota, winters and summers may be up to 6°C and 4°C warmer, respectively, at the end of the 21st century.
- Spring precipitation may increase by more than 1 mm d^{-1} over northern Minnesota.
- Snow height may decrease by more than 0.5 meters. Number of snow days per year may decrease by up to 60.

Index Terms: 3355, 1637, 3305, 3309, 3322

Keywords: Dynamical Downscaling; Weather Research and Forecasting (WRF) model; Regional Climate Change over Midwestern USA; Cropland Simulations

Abstract

Minnesota is the U.S. state with the strongest winter warming in the contiguous United States. We performed regional climate projections at 10 km horizontal resolution using the WRF model forced by an ensemble of eight CMIP5 GCMs. The selected GCMs have previously been found to be in relatively good agreement with observations compared to other members of the CMIP5 model ensemble. Our projections suggest ongoing warming in all seasons, especially in winter, as well as shallower snow cover and fewer days with snow cover. On the other hand, we expect significant increases in spring and early summer heavy precipitation events. Our comparisons between different time slices and two different emission scenarios indicate a climate for the state of Minnesota at the end of the 21st century that is significantly different from what has been observed by the end of the 20th century. Winters and summers are expected to be up to 6°C and 4°C warmer, respectively, over northern and central Minnesota and spring precipitation may increase by more than 1 mm d^{-1} over northern Minnesota. Especially over the central part of the state, winter snow height is suggested to decrease by more than 0.5 meters and the number of days per year

with snow height of more than 0.0254 meters (one inch) is expected to decrease by up to 60.

Plain Language Summary

Minnesota is the U.S. state with the strongest winter warming in the contiguous United States. We performed regional projections of the climate over the counties of Minnesota for the middle and end of the 21st century. For this, we selected the results from eight recent global climate model projections to calculate climate data over 10 km by 10 km areas with a regional climate model. Our comparisons indicate that the future climate for the state of Minnesota is significantly different from what has been observed by the end of the 20th century. Especially over northern and central Minnesota, winters and summers are expected to be up to 6°C and 4°C warmer, respectively, at the end of the 21st century. Spring precipitation may increase by more than 1 mm d^{-1} over northern Minnesota. Over the central part of the state, winter snow height is suggested to decrease by more than 0.5 meters. The number of days per year with snow height of more than 0.0254 meters (one inch) is expected to decrease by up to 60. These results are expected to influence regional decision-making related to agriculture, infrastructure, water resources, and other sectors.

1. Introduction

For almost a century, surface warming has had its largest amplitude in the higher latitudes of the Northern Hemisphere (Callendar 1938). Over the last several decades, the Arctic region has on average warmed at twice the rate as the rest of the planet, and with anthropogenic climate change, it may warm an additional 4-8°C by the end of this century (IPCC 2013). The U.S. state of Minnesota is strongly affected by this Arctic warming, particularly during winter, when the influence of Arctic air is most dominant and when reduced snow cover reduces albedo. Minnesota's winter warming is the strongest among the 48 contiguous United States (NCEI 2021). Future projections indicate ongoing warming as well as significant increases in spring and early summer heavy precipitation events over the north-central U.S. by the end of this century (Harding and Snyder 2014).

Despite the clear signals of increased temperature and precipitation in models of future climate, the large-scale outputs of general circulation models (GCM) are difficult to integrate into regional, state, and local planning, where climate information is required by decision makers over smaller areas such as individual watersheds and counties. GCMs typically have resolutions coarser than 100 km, which is insufficient for these applications (Zorita and von Storch 1999; Boé et al. 2007). Differentiating the impacts of climate change at finer spatial scales is particularly important and challenging in Minnesota, where many days of snow cover and many small-scale open water sources, such as lakes and rivers all contribute to variation on the ground. In order to provide reasonable climate projections over Minnesota on the regional scale, we dynamically downscaled GCM projections from an eight-model ensemble to a higher spatial resolution

by nesting a finer scale regional climate model (RCM) (Giorgi and Gutowski 2015) .

1. **Methods**

We use a dynamical downscaling approach based on nesting GCM input data with the Weather Research and Forecasting (WRF) RCM (Skamarock et al. 2008) coupled to the Community Land Model (CLM) (Dai et al. 2003) with a dynamic crop module. This model version, also known as WRF-CLM4crop, has previously been described by Lu et al. (2015) and Harding et al. (2016). From more than 40 available GCMs, we selected eight that provide all necessary prognostic variables and that show reliable large-scale results over the Midwestern USA (Table 1; Harding et al. 2013). Boundary conditions include 6-hourly prognostic variables such as temperature, wind speed and direction, specific humidity, and geopotential height from the Coupled Model Intercomparison Project 5 (CMIP5) GCM archive (Taylor et al. 2012) at the Earth System Grid (Williams et al. 2009). Vegetation, soil, and other land surface parameters over the WRF domains are taken from the annual cycle of the Moderate-resolution Imaging Spectroradiometer (MODIS) satellite product at 30-second horizontal resolution (Zhang et al. 2006) and kept consistent between all simulations.

Our downscaling approach is based on one-way nesting between the global and regional domains, and two-way nesting between the two regional domains, so our RCM results cannot modify the global domain. Our regional domains comprise an outer nest over a large portion of North America at 50 km grid-cell horizontal resolution and an inner nest over Minnesota and adjacent areas at 10 km grid-cell horizontal resolution (Fig. 1). These two nests are connected via two-way nesting and thus influence one other. We compute downscaled regional climate projections for the historical period of 1980-1999; from the RCP4.5 scenario, which assumes a moderate amount of mitigation of GHG emissions (van Vuuren et al. 2011) for two 20-year periods of the 21st century (2040-2059 and 2080-2099); and from the RCP8.5 scenario, which assumes only a minimum of mitigation, for the 2080-2099 period (Riahi et al. 2011). For the state of Minnesota and surrounding regions, we use WRF to generate hourly averages of the following surface variables: 2-m air temperature, 2-m humidity, and 10-m wind speed and direction, precipitation, downward solar radiation, net radiation, latent, sensible, and ground heat fluxes, snow height, and soil temperature and moisture content at 10 layers to a depth of 2.5 m.

We perform a simple linear-scaling bias-correction (Teutschbein and Seibert 2012) to surface air temperature and precipitation as described in equations 1-4 in Shrestha et al. (2017) using monthly mean observations as reported by the PRISM group (Daly et al. 2017) . We compare observations and WRF-simulated values from runs forced with each GCM for each monthly average (i.e., the average temperature difference over every January from 1980-1999 is calculated to receive one offset value for January at each grid point). Precipitation values are scaled by dividing monthly model values by observational averages for 1981-2000. The 2-m air temperature and precipitation error corrections are

then applied to data from each WRF run for each future scenario. Variables other than air temperature and precipitation are not corrected because of lack of available observations. The prognostic variables for CCSM4 and CMCC-CM were previously bias-corrected, so their historical multi-year monthly means match reanalysis data, as described in Bruyère et al. (2014). We apply the same bias correction to the prognostic variables of all future scenarios for these two models.

In addition to analyzing WRF results forced from each GCM, we analyze the multi-model ensemble (MME) of each variable averaged over all WRF-forced runs from all GCMs. Individual years of the simulations are treated as individual ensemble members in analyses, which allows a robust statistical analysis with 160 ensemble members per scenario. The advantage of this approach is that an MME with eight downscaled models should be considered as more reliable than individual model results, as previously demonstrated by Pincus et al. (2008).

1. **Results and Discussion**

   (a) *Statewide area averages*

The statewide area averages are computed by averaging over all grid cells with more than 50% of their area inside the state. The seasonal cycle of these values, especially precipitation, is generally improved by physical downscaling (Mendez et al. 2020). Bias correction based on linear scaling retains the interannual variability (the gray lines in Fig. 2) but forces each multi-year monthly average for each GCM-forced WRF run in the historical simulations to equal the PRISM observations. Linear scaling assumes that this offset carries through to the climate simulations of the future, so the simulations will now diverge in their calculations of these variables, and the variability increases for simulations of future climate (Figs. 2 & 3).

MME 2-m temperature increases in each scenario compared to the historical period, particularly in winter (Fig. 2). WRF simulates less future warming than the MME when forced with MRI-CGCM3 and GFDL-ESM2M, and generally stronger warming when forced with MIROC5 and IPSL-CM5A-LR. Simulated warming forced with bcc-csm1-1, CCSM4, CMCC-CM, and CNRM-CM5 is relatively close to the MME.

Simulated precipitation variability (Fig. 3) increases in spring and summer, especially in the late 21st century. Early summer MME rainfall increases mid-century and in RCP8.5 late-century, while fall MME rainfall increases in both scenarios in late-century. There is a very small increase in winter MME precipitation in all scenarios. The WRF forcing with GFDL-ESM2M and MRI-CGCM3 shows the strongest increases, whereas forcing with MIROC5 shows decreases from late spring through early fall in all scenarios. WRF-forced simulations of precipitation from CMCC-CM are notably different from those from other models, with large increases in fall for both late-21st-century simulations. As with temperature, WRF forcing of precipitation from bcc-csm1-1, CCSM4, and CNRM-CM5 is closest to the MME.

1. *Spatial distributions*

Twenty-year average winter (Figure 4a) and summer (Figure 5a) MME 2-meter temperatures illustrate the strong north-south temperature gradient in the state as seen in the historic period simulation of temperature. Winter (Figure 4b-d) MME anomalies show that temperature increases are stronger along the northern border (Figure 4b) in mid-century, throughout much of the northern half of the state in RCP4.5 by end of century (Figure 4c), and throughout most of the northern half of the state in RCP8.5 (Figure 4d). This increased rate of warming in the north is due to both synoptic-scale warming as well as reduced albedo from reduced snow cover (not shown), which results in increases in average winter temperature ranging from ~1 °C by mid-century to 6 °C by end of century in RCP8.5 (Figure 4d). Observations of winter average temperature across Minnesota show trends in warming (Runkle et al. 2017; their Fig. 1) and these simulations continue the trend. Increases in summer average temperature show a more homogeneous increase across the state that ranges from ~1 °C by mid-century (Figure 5b) to 5 °C by end of century in RCP8.5 (Figure 5d). These simulated future increases in summer average temperature contrast with observations of summer average temperature across the state that do not show a significant trend in the historical record (Runkle et al. 2017; their Fig. 2a).

According to the statewide average analysis (Figure 3), most of the change in future precipitation occurs in spring and early summer; therefore, we analyze spring average MME precipitation (rain and snow water equivalent) here. Spring average MME precipitation across Minnesota shows a gradient with the wettest areas in the southeast portion of the state and driest in the northwest (Fig. 6a). Simulated precipitation changes by mid-century differs among WRF runs with some runs showing spring increases (e.g., driven with IPSL) and some showing decreases (e.g., driven with MIROC5 and GFDL; Figure 3b), which together result in no significant changes in spring average precipitation across the state (Figs. 6b). By end of century, spring precipitation is projected to increase slightly in the far north of the state in RCP4.5 (Figure 6c) and by up to 1 mm d^{-1} in the northern half of the state as well as the southern portion of the domain in Iowa in RCP8.5 (Figure 6d). Because the greatest increase in rainfall is projected to occur in the northern part of the state, spring average rainfall across the state will become more homogeneous. Winter average MME precipitation is projected to increase slightly though statistically significant by end of century, by 0.25 mm d^{-1} in RCP8.5 (not shown). We adjusted the degrees of freedom in our statistical tests to account for lag-1 auto-correlation in our data, according to Wilks (2011).

Average winter MME snow height generally increases with latitude across the state, however, there is a lobe of lower snow heights stretching northward on the far western side of the state (Figure 7a). Despite the currently observed and projected increases in precipitation, snow height is projected to decrease across the state except in the northernmost region during the 21st century (Fig. 7b-d) because of increased surface air temperature. Strongest decreases in snow

height are projected to occur in central Minnesota, where average snow height is expected to decrease by up to 50% by the middle of the 21st century (Figure 7b). By the end of the 21st century under RCP8.5, this change is expected to also cover southern Minnesota and the maximum reduction in snow height reaches more than 0.5 m. While snow height over the northernmost part of the state remains unchanged, the simulations show significant decreases in snow height along the Minnesota North Shore and into much of Wisconsin exceeding 0.5 m. These regions include part of the U.S. National Forest system and are at risk for decreasing revenues in winter recreation as well as threats to ecosystem health from pests that may survive warmer winters (Govindan and Hutchison 2020; Venette and Hutchison 2021).

The average MME number of days per year when snow height meets or exceeds a threshold of 0.0254 m (equivalent to one inch) follows a similar pattern as average MME snow height (Figure 8a). Warmer winters result in fewer days with snow cover on the ground. Significant decreases in days per year with snow cover above one inch are found over central and southeast Minnesota and western Wisconsin of up to 40 days per year by mid-century (Figure 8b). By end of century with RCP8.5, there are up to 60 fewer days of snow cover in Minnesota and more than 70 fewer days in central Wisconsin (Figure 8d).

The goal of this study is to develop a dynamically downscaled climate dataset for Minnesota to be used for impact studies. This dataset will be useful if it provides value to previously developed, well-tested datasets (i.e., is higher resolution while broadly agreeing with other projections). While there are differences in the number of GCMs, time periods, and downscaling methods between our study and that of the National Climate Assessment (NCA), our results are consistent in magnitudes and patterns. For example, our statewide average annual temperature increases (Figure 2.b-d) agree broadly with Midwest average projected increases for RCP4.5 by mid-century (2.3 °C), and for end of century for RCP4.5 (3.1 °C) and RCP8.5 (5.3 °C) in Table 6.4 of the NCA (Vose et al. 2017).

The benefits of downscaling are really highlighted for a variable like precipitation that is strongly variable in space and time and for which variability is projected to increase in the future. Like our analysis, the NCA found more significant changes in projected precipitation in winter and spring than in fall and summer (Easterling et al. 2017). While their analysis shows a homogeneous increase in winter and spring precipitation for RCP8.5 by the end of the century of about 20%, we found a smaller though statistically significant increase in winter precipitation and more spatial variability in projected spring precipitation. Our projected RCP8.5 end of century spring precipitation ranges from no statistically significant change in the southern portion of the state to a 12-30% increase in the central region and a 30-60% increase in the north. While our analysis provides a more detailed projection of future precipitation than the NCA, we note that there are limitations to our analysis because of the single model used to downscale data and the single method of bias correction we employed (Laux

et al. 2021). Future studies will examine alternate methods of bias correction of this dataset.

The data presented here are immediately useful for impact studies of agricultural, energy, economic, and other ecosystem service sectors of Minnesota, and will be a baseline for comparison with future downscaling efforts of CMIP6 (Stouffer et al. 2017). Multi-model ensemble values of temperature and precipitation are available at a variety of user-defined domains from climate.umn.edu (The Minnesota Department of Natural Resources Climate Trends Tool) and raw data are available by request.

1. Conclusions

The present study describes a high-resolution regional climate modeling effort over the U.S. state of Minnesota that is already providing input for various projects including improved projections of weather extremes, management of infrastructure, industry, and water resources (Noe et al. 2019) as well as the tracking of invasive species (Govindan and Hutchison 2020; Venette and Hutchison 2021). This state-level downscaling effort links climate projections to decision making within regional communities. Snow cover simulations emphasize the need of detailed modeling efforts of the hydrological cycle especially over high-latitude climates.

Acknowledgments

CMIP5 data were obtained from the Earth System Grid at https://www.earthsystemgrid.org. Temperature and precipitation observations were made available by the PRISM group at http://www.prism.oregonstate.edu. The authors acknowledge Keith J. Harding and the Minnesota Supercomputing Institute at the University of Minnesota for providing resources that contributed to the research results reported within this paper (http://www.msi.umn.edu). Funding for this project was provided by the Minnesota Invasive Terrestrial Plants and Pests Center (http://www.mitppc.umn.edu) and the Minnesota Environment and Natural Resources Trust Fund (http://www.legacy.mn.gov) as recommended by the Legislative-Citizen Commission on Minnesota Resources. The Trust Fund is a permanent fund constitutionally established by the citizens of Minnesota to assist in the protection, conservation, preservation, and enhancement of the state's air, water, land, fish, wildlife, and other natural resources. Currently, 40% of net Minnesota State Lottery proceeds are dedicated to growing the Trust Fund and ensuring future benefits for Minnesota's environment and natural resources.

References

Boé, J., L. Terray, F. Habets, and E. Martin, 2007: Statistical and dynamical downscaling of the Seine basin climate for hydro-meteorological studies. *Int. J. Climatol.*, **27**, 1643–1655, https://doi.org/10.1002/joc.1602.Bruyère, C. L., J. M. Done, G. J. Holland, and S. Fredrick, 2014: Bias corrections of global models for regional climate simulations of high-impact weather. *Clim. Dyn.*, **43**,

1847–1856, https://doi.org/10.1007/s00382-013-2011-6.Callendar, G. S., 1938: The artificial production of carbon dioxide and its influence on temperature. *Q. J. R. Meteorol. Soc.*, **64**, 223–240, https://doi.org/10.1002/qj.49706427503.Dai, Y., and Coauthors, 2003: The common land model. *Bull. Am. Meteorol. Soc.*, **84**, 1013–1023, https://doi.org/10.1175/BAMS-84-8-1013.Daly, C., M. E. Slater, J. A. Roberti, S. H. Laseter, and L. W. Swift, 2017: High-resolution precipitation mapping in a mountainous watershed: ground truth for evaluating uncertainty in a national precipitation dataset. *Int. J. Climatol.*, **37**, 124–137, https://doi.org/10.1002/joc.4986.Dufresne, J.-L., and S. Bony, 2008: An assessment of the primary sources of spread of global warming estimates from coupled atmosphere–ocean models. *J. Climate*, **21**, 5135–5144, https://doi.org/10.1175/2008jcli2239.1.Dunne, J. P., and Coauthors, 2012: GFDL's ESM2 Global Coupled Climate–Carbon Earth System Models. Part I: Physical Formulation and Baseline Simulation Characteristics. *J. Climate*, **25**, 6646–6665, https://doi.org/10.1175/JCLI-D-11-00560.1.Easterling, D. R., and Coauthors, 2017: *Ch. 7: Precipitation Change in the United States. Climate Science Special Report: Fourth National Climate Assessment, Volume I.*Gent, P. R., and Coauthors, 2011: The Community Climate System Model version 4. *J. Climate*, **24**, 4973–4991, https://doi.org/10.1175/2011jcli4083.1.Giorgi, F., and W. J. Gutowski, 2015: Regional Dynamical Downscaling and the CORDEX Initiative. *Annu. Rev. Environ. Resour.*, **40**, 467–490, https://doi.org/10.1146/annurev-environ-102014-021217.Govindan, B. N., and W. D. Hutchison, 2020: Influence of Temperature on Age-Stage, Two-Sex Life Tables for a Minnesota-Acclimated Population of the Brown Marmorated Stink Bug (Halyomorpha halys). *Insects*, **11**, 108, https://doi.org/10.3390/insects11020108.Harding, K. J., and P. K. Snyder, 2014: Examining future changes in the character of Central U.S. warm-season precipitation using dynamical downscaling. *J. Geophys. Res. Atmos.*, **119**, 13,116-13,136, https://doi.org/10.1002/2014JD022575.Harding, K. J., P. K. Snyder, and S. Liess, 2013: Use of dynamical downscaling to improve the simulation of Central U.S. warm season precipitation in CMIP5 models. *J. Geophys. Res. Atmos.*, **118**, 12,512-522,536, https://doi.org/10.1002/2013JD019994.Harding, K. J., T. E. Twine, A. VanLoocke, J. E. Bagley, and J. Hill, 2016: Impacts of second-generation biofuel feedstock production in the central U.S. on the hydrologic cycle and global warming mitigation potential. *Geophys. Res. Lett.*, **43**, 10,773-10,781, https://doi.org/10.1002/2016GL069981.IPCC, 2013: Climate Change 2013: The Physical Science Basis. Contribution of Working Group I to the Fifth Assessment Report of the Intergovernmental Panel on Climate Change. T.F. Stocker et al., Eds., Cambridge University Press, p. 1535 pp.Laux, P., and Coauthors, 2021: To bias correct or not to bias correct? An agricultural impact modelers' perspective on regional climate model data. *Agric. For. Meteorol.*, **304–305**, 108406, https://doi.org/10.1016/j.agrformet.2021.108406.Lu, Y., J. Jin, and L. M. Kueppers, 2015: Crop growth and irrigation interact to influence surface fluxes in a regional climate - cropland model (WRF3 . 3 - CLM4crop). *Clim. Dyn.*, **45**, 3347–3363, https://doi.org/10.1007/s00382-015-

2543-z.Mendez, M., B. Maathuis, D. Hein-Griggs, and L.-F. Alvarado-Gamboa, 2020: Performance Evaluation of Bias Correction Methods for Climate Change Monthly Precipitation Projections over Costa Rica. *Water*, **12**, 482, https://doi.org/10.3390/w12020482.NCEI, 2021: *National Trends Temperature, Precipitation, and Drought National Centers for Environmental Information (NCEI).* https://www.ncdc.noaa.gov/temp-and-precip/us-trends/tavg/win (Accessed February 20, 2021).Noe, R., B. Keeler, T. Twine, K. Brauman, T. Mayer, and M. Rogers, 2019: *Climate change projections for improved management of infrastructure, industry, and water resources in Minnesota.* http://hdl.handle.net/11299/209130 (Accessed March 25, 2020).Pincus, R., C. P. Batstone, R. J. P. Hofmann, K. E. Taylor, and P. J. Glecker, 2008: Evaluating the present-day simulation of clouds, precipitation, and radiation in climate models. *J. Geophys. Res.*, **113**, D14209, https://doi.org/10.1029/2007jd009334.Riahi, K., and Coauthors, 2011: RCP 8.5—A scenario of comparatively high greenhouse gas emissions. *Clim. Change*, **109**, 33–57, https://doi.org/10.1007/s10584-011-0149-y.Runkle, J., K. Kunkel, R. Frankson, D. Easterling, and S. Champion, 2017: *Minnesota State Climate Summary. NOAA Technical Report NESDIS 149-MN.* 4 pp. https://statesummaries.ncics.org/chapter/mn/.Scoccimarro, E., and Coauthors, 2011: Effects of tropical cyclones on ocean heat transport in a high-resolution coupled general circulation model. *J. Climate*, **24**, 4368–4384, https://doi.org/10.1175/2011JCLI4104.1.Shrestha, M., S. C. Acharya, and P. K. Shrestha, 2017: Bias correction of climate models for hydrological modelling – are simple methods still useful? *Meteorol. Appl.*, **24**, 531–539, https://doi.org/10.1002/met.1655.Skamarock, W. C., and Coauthors, 2008: *A description of the Advanced Research WRF version 3.* National Center for Atmospheric Research, 125 pp.Stouffer, R. J., V. Eyring, G. A. Meehl, S. Bony, C. Senior, B. Stevens, and K. E. Taylor, 2017: CMIP5 scientific gaps and recommendations for CMIP6. *Bull. Am. Meteorol. Soc.*, **98**, 95–105, https://doi.org/10.1175/BAMS-D-15-00013.1.Taylor, K. E., R. J. Stouffer, and G. A. Meehl, 2012: An overview of CMIP5 and the experiment design. *Bull. Am. Meteorol. Soc.*, **93**, 485–498, https://doi.org/10.1175/BAMS-D-11-00094.1.Teutschbein, C., and J. Seibert, 2012: Bias correction of regional climate model simulations for hydrological climate-change impact studies: Review and evaluation of different methods. *J. Hydrol.*, **456**–**457**, 12–29, https://doi.org/10.1016/j.jhydrol.2012.05.052.Venette, R. C., and W. D. Hutchison, 2021: Invasive Insect Species: Global Challenges, Strategies & Opportunities. *Front. Insect Sci.*, **1**, 650520, https://doi.org/10.3389/finsc.2021.650520.Voldoire, A., and Coauthors, 2012: The CNRM-CM5.1 global climate model: description and basic evaluation. *Clim. Dyn.*, 1–31, https://doi.org/10.1007/s00382-011-1259-y.Vose, R. S., D. R. Easterling, K. E. Kunkel, A. N. LeGrande, and M. F. Wehner, 2017: *Ch. 6: Temperature Changes in the United States. Climate Science Special Report: Fourth National Climate Assessment, Volume I.*van Vuuren, D. P., and Coauthors, 2011: The representative concentration pathways: an overview. *Clim. Change*, **109**, 5–31, https://doi.org/10.1007/s10584-011-

0148-z.Watanabe, M., and Coauthors, 2010: Improved climate simulation by MIROC5: mean states, variability, and climate sensitivity. *J. Climate*, **23**, 6312–6335, https://doi.org/10.1175/2010jcli3679.1.Wilks, D. S., 2011: *Statistical Methods in the Atmospheric Sciences*. 3rd ed. R. Dmowska, D. Hartmann, and H.T. Rossby, Eds. Academic Press, 676 pp.Williams, D. N., and Coauthors, 2009: The earth system grid: Enabling access to multimodel climate simulation data. *Bull. Am. Meteorol. Soc.*, **90**, 195–205, https://doi.org/10.1175/2008BAMS2459.1.Wu, T., and Coauthors, 2010: The Beijing Climate Center atmospheric general circulation model: description and its performance for the present-day climate. *Clim. Dyn.*, **34**, 123–147, https://doi.org/10.1007/s00382-008-0487-2.Yukimoto, S., and Coauthors, 2012: A new global climate model of the Meteorological Research Institute: MRI-CGCM3 - Model Description and Basic Performance -. *J. Meteorol. Soc. Japan*, **90A**, 23–64, https://doi.org/10.2151/jmsj.2012-A02.Zhang, X., M. A. Friedl, and C. B. Schaaf, 2006: Global vegetation phenology from Moderate Resolution Imaging Spectroradiometer (MODIS): Evaluation of global patterns and comparison with in situ measurements. *J. Geophys. Res.*, **111**, G04017, https://doi.org/10.1029/2006jg000217.Zorita, E., and H. von Storch, 1999: The Analog Method as a Simple Statistical Downscaling Technique: Comparison with More Complicated Methods. *J. Climate*, **12**, 2474–2489, https://doi.org/10.1175/1520-0442(1999)012<2474:TAMAAS>2.0.CO;2.

Table 1. List of GCMs for boundary conditions.

Model	**Institution**	**Resolution [°]**	**Reference**
bcc-csm1-1	BCC (China)	1 x 1.33	(Wu et al. 2010)
CCSM4	NCAR (USA)	0.9 x 1.25	(Gent et al. 2011)
CMCC-CM	CMCC (Italy)	0.75 x 0.75	(Scoccimarro et al. 2011)
CNRM-CM5	CNRM-CERFACS (France)	1.5 x 1.5	(Voldoire et al. 2012)
GFDL-ESM2M	NOAA-GFDL (USA)	2 x 2.5	(Dunne et al. 2012)
IPSL-CM5A-LR	IPSL (France)	1.875 x 3.75	(Dufresne and Bony 2008)
MIROC5	MIROC (Japan)	2.8 x 2.8	(Watanabe et al. 2010)
MRI-CGCM3	MRI (Japan)	1.125 x 1.125	(Yukimoto et al. 2012)

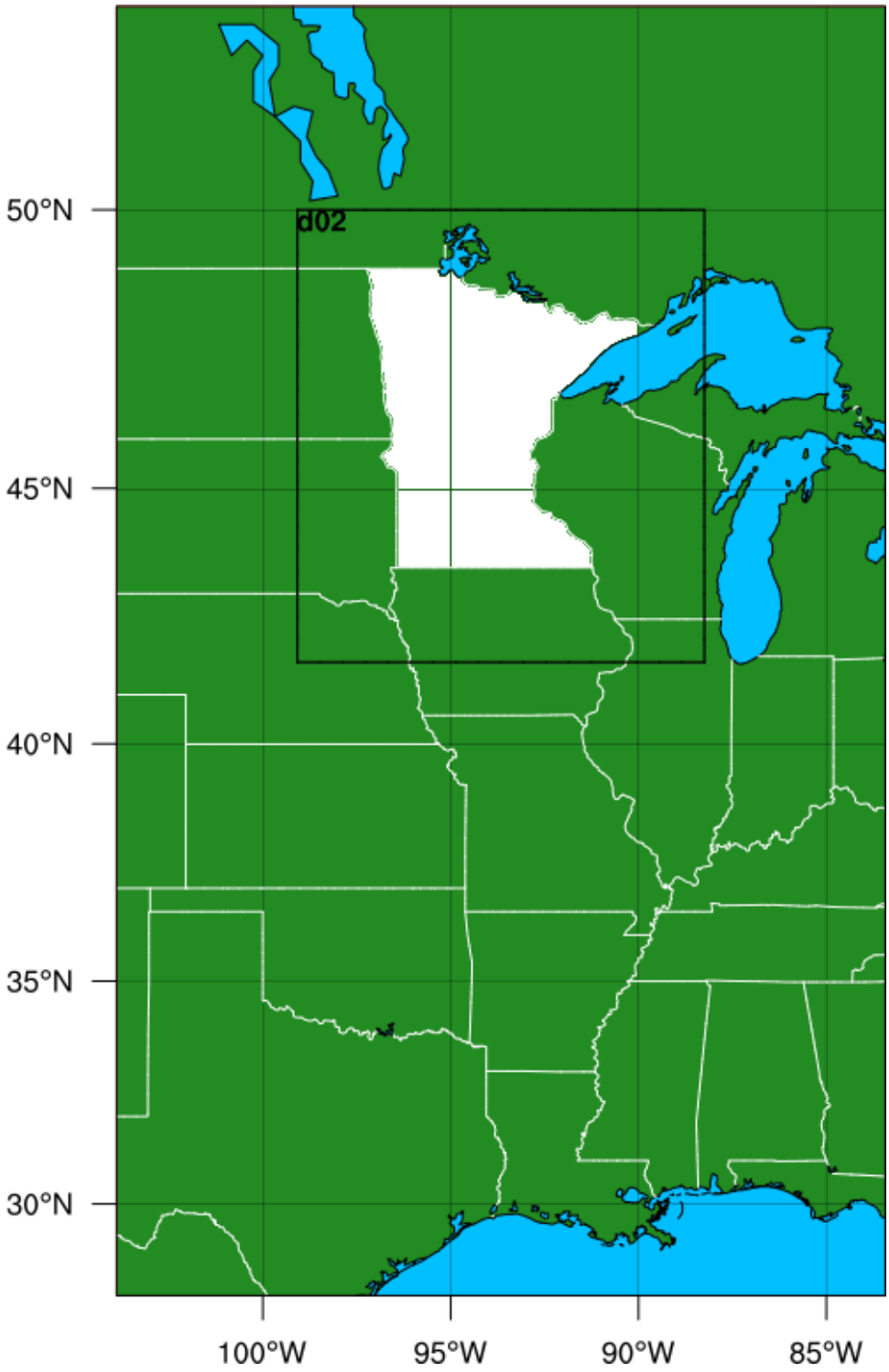
d02
50°N
45°N
40°N
35°N
30°N
100°W
95°W
90°W
85°W

Fig. 1: The outer (complete map) and inner grid (black frame) used for climate projections. The state of Minnesota is marked in white.

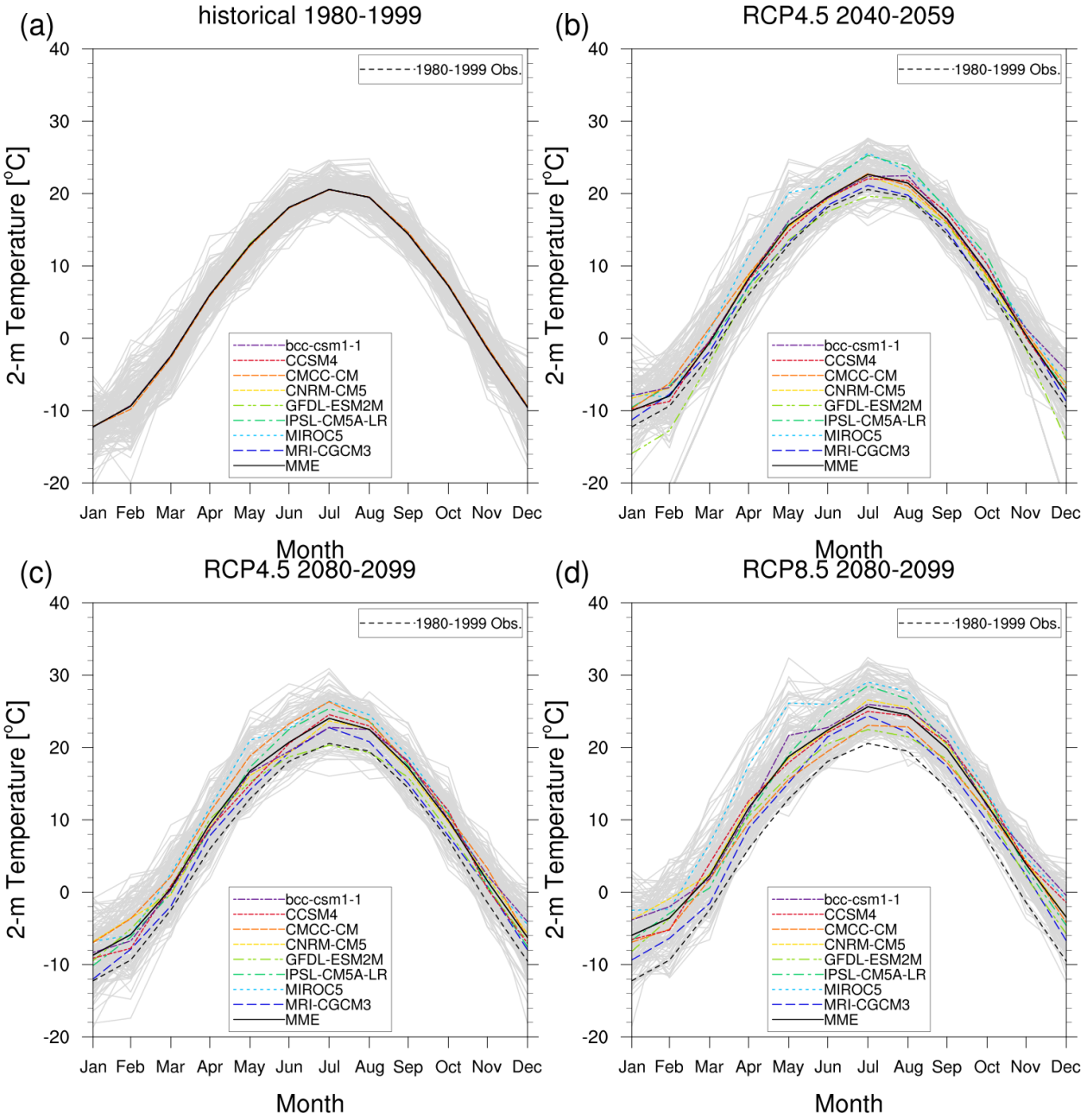

Fig. 2: 1980-1999 monthly average 2-meter air temperature averaged over every grid cell within that state of Minnesota for each WRF-downscaled GCM (colors),

the multi-model mean (MME; black line), and the PRISM dataset (dashed line). Also shown are each of the WRF 20-year runs for all GCMS (160 realizations; gray lines).

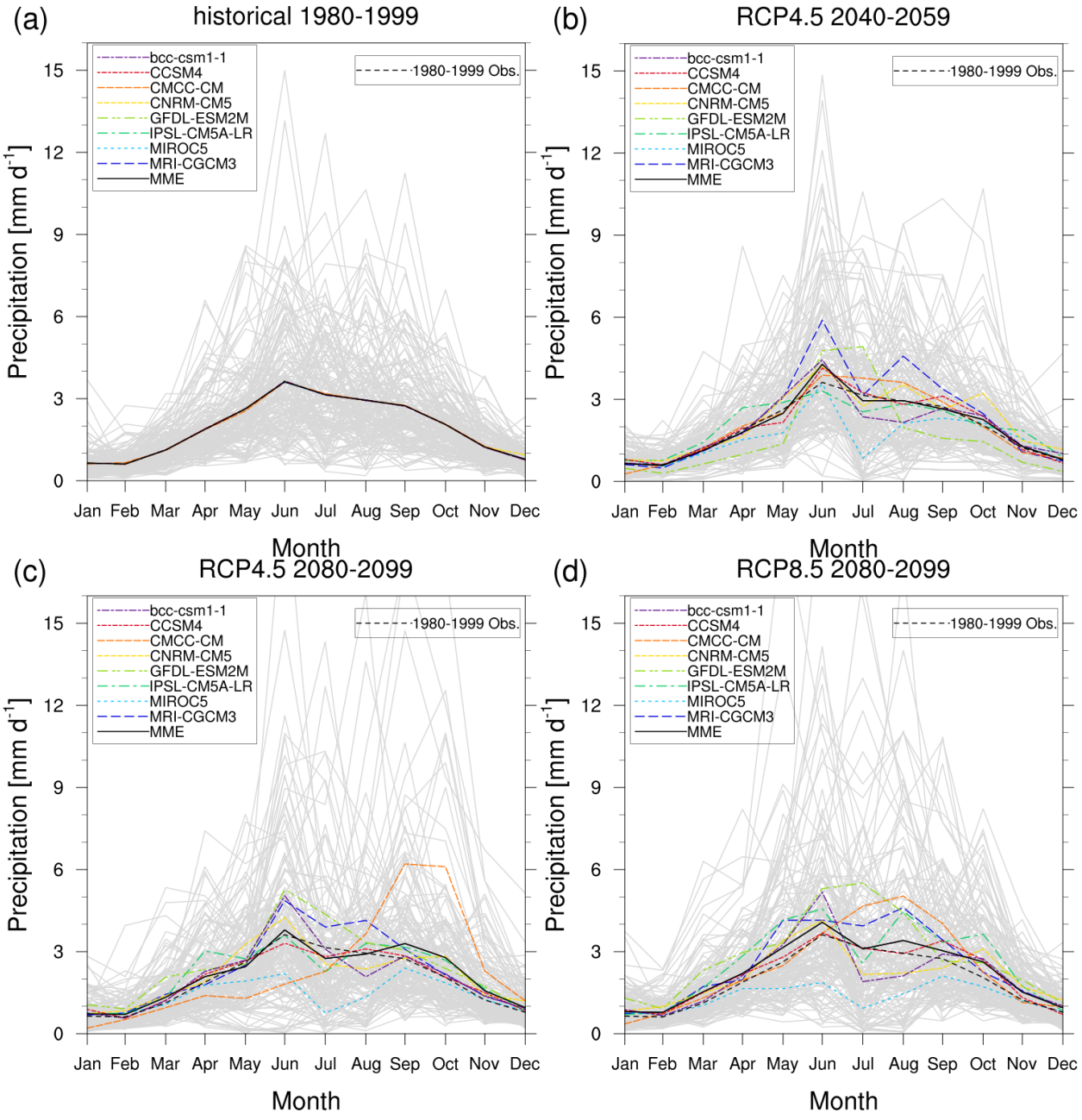

Fig. 3: As Fig. 2, but for precipitation.

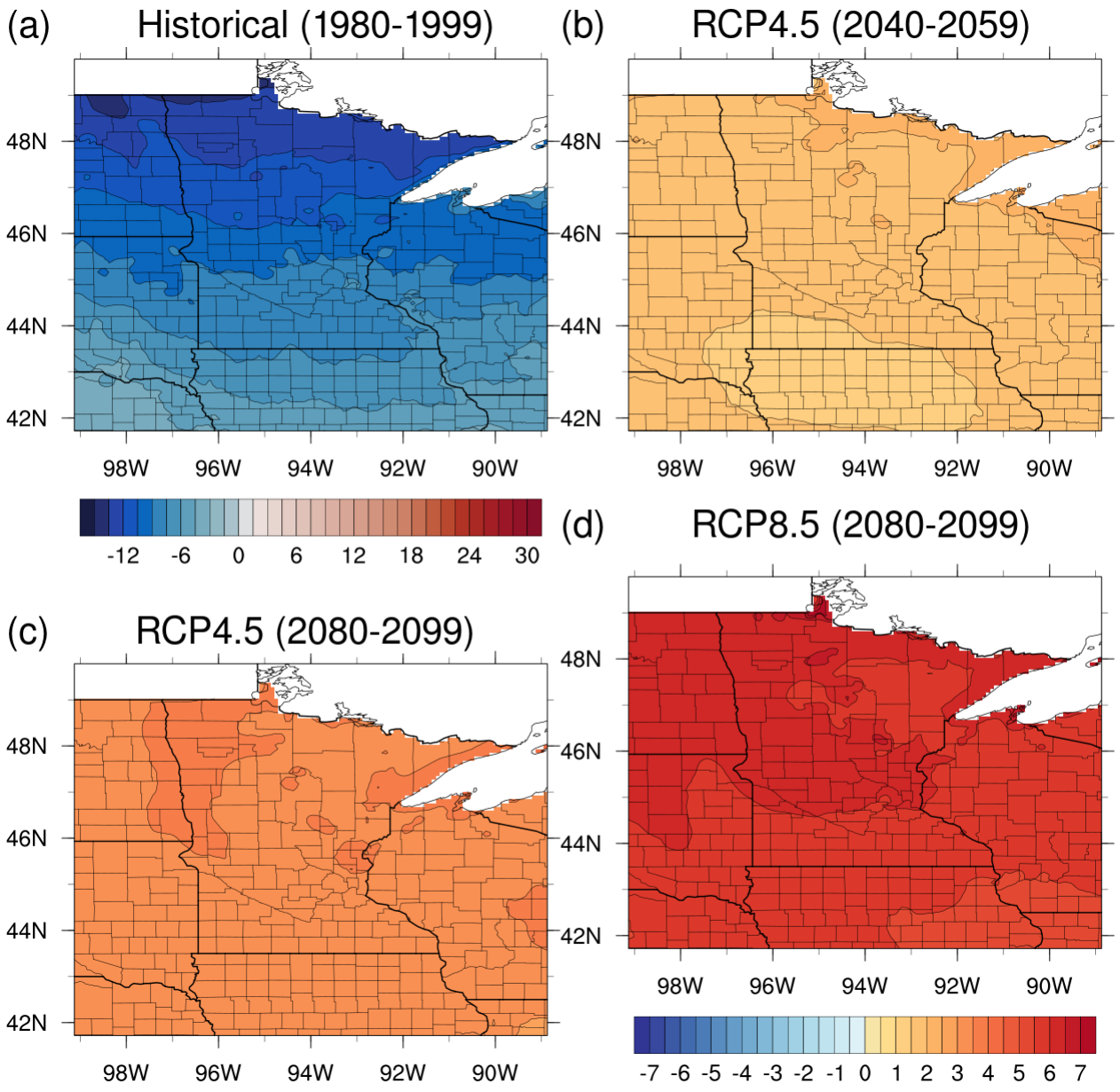

Fig. 4: Average winter (December-February) MME 2-meter air temperature in °C for (a) historical simulations and (b-d) anomalies of each RCP scenario compared to the historical period. Shading in (b-d) indicates statistically significant changes over U.S. land points at the 95% confidence interval. Please note that there is a different color bar for (a) than for (b-d).

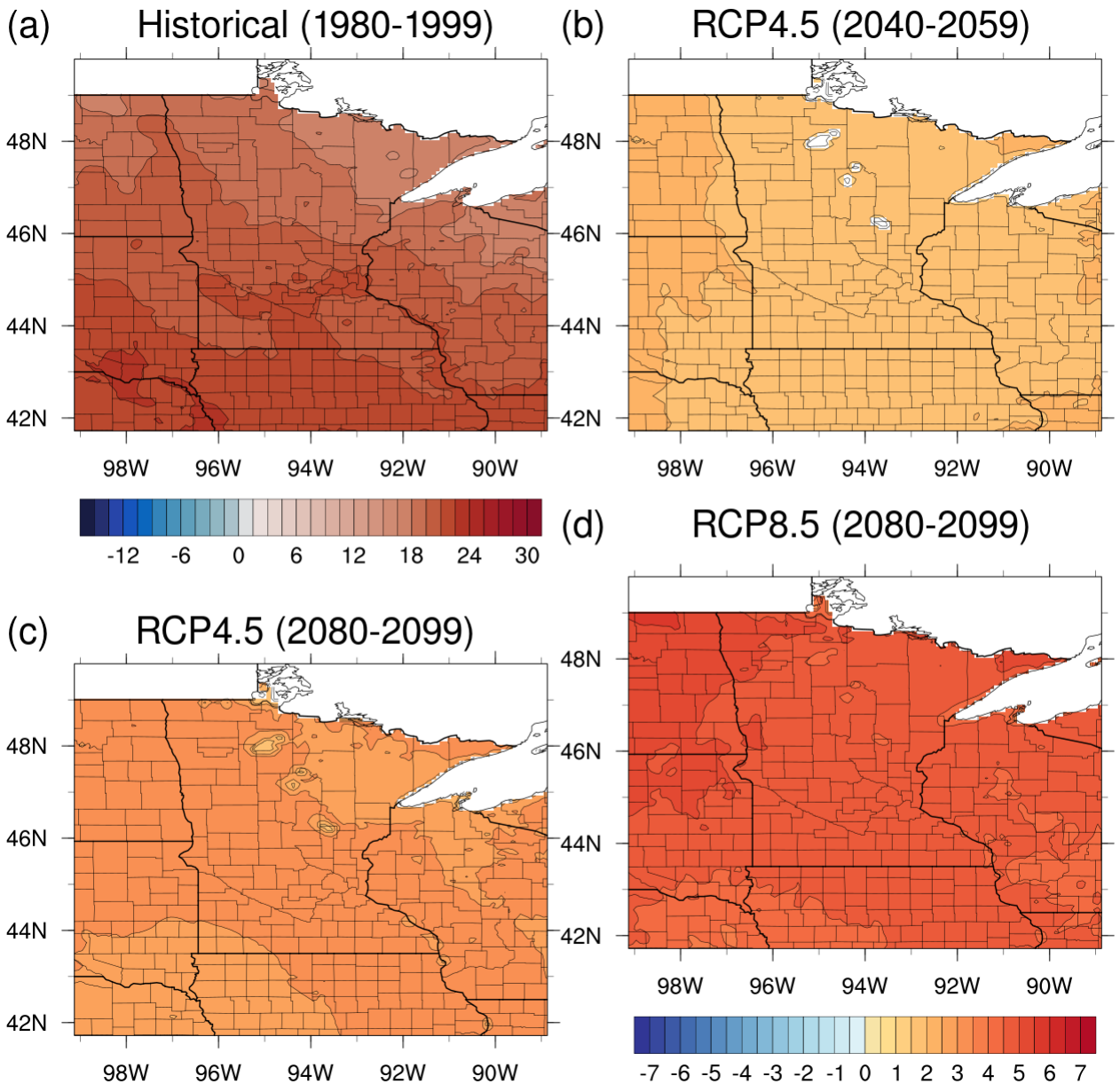

Fig. 5: As Fig. 4, but for summer (June-August).

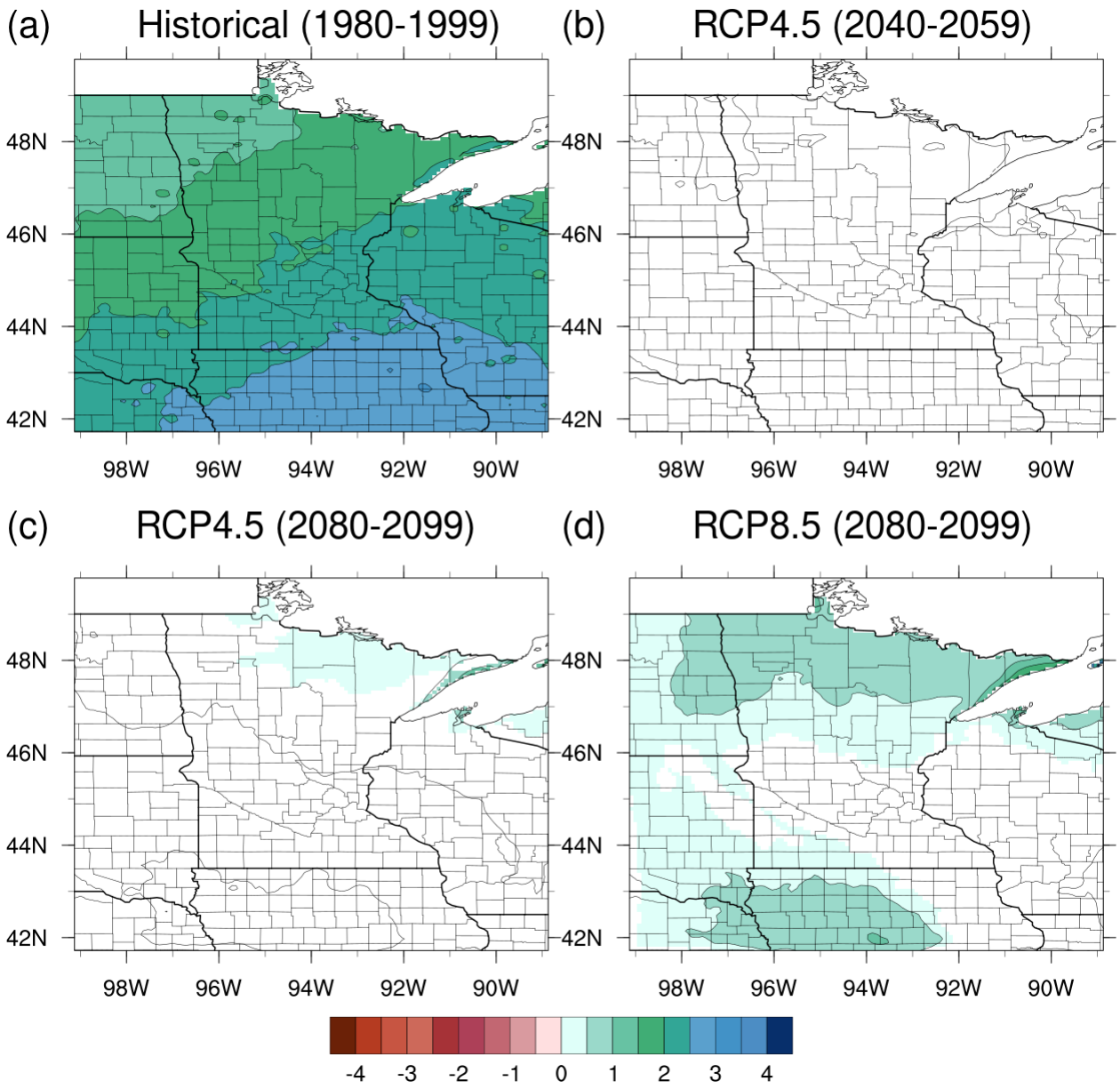

Fig. 6: As Fig. 4, but for precipitation and precipitation anomalies in mm d^{-1} in spring (March-May). Color bar is valid for all panels.

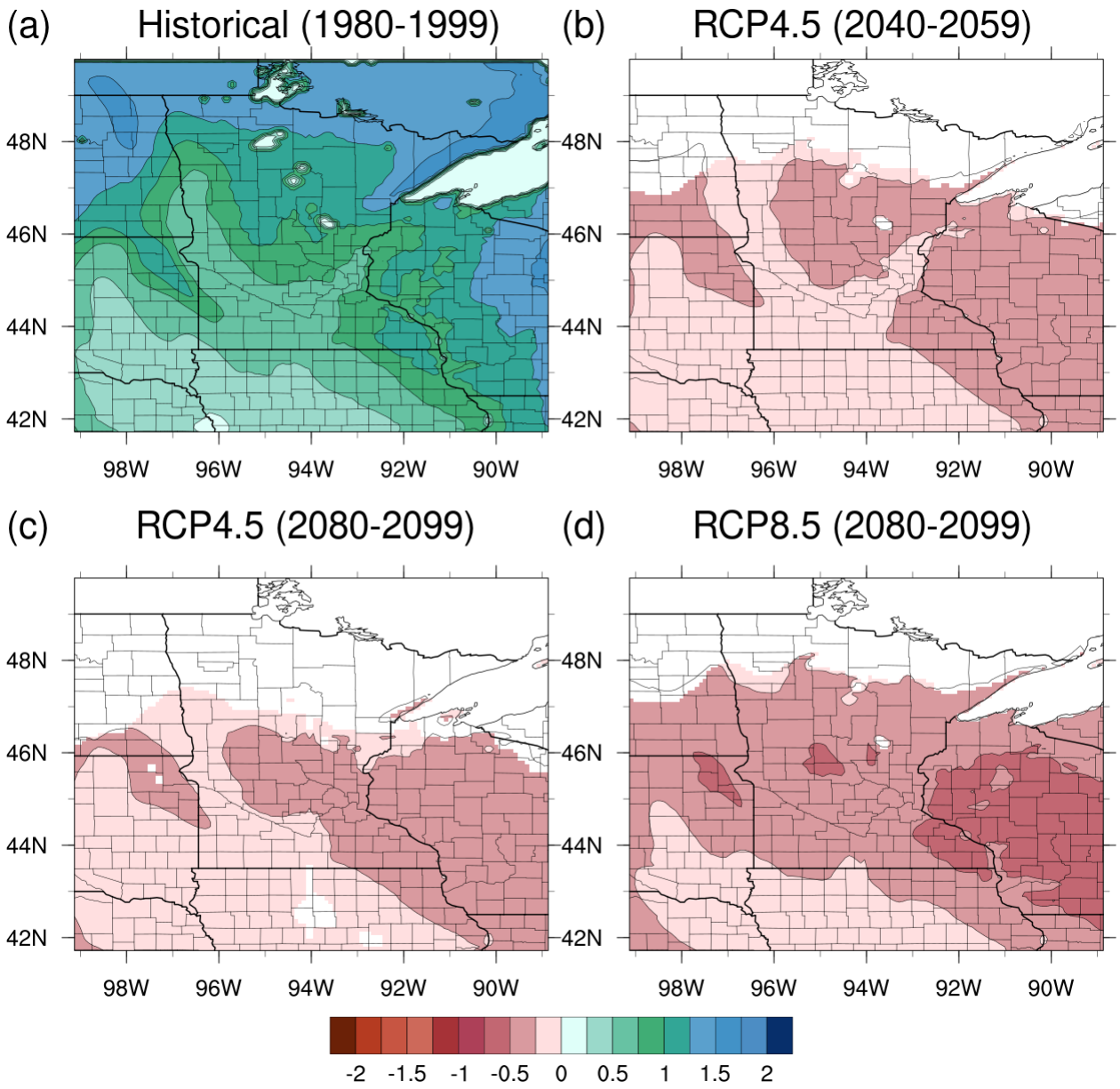

Fig. 7: As Fig. 4, but for MME snow height and snow height anomalies (m) in winter (December-February). Color bar is valid for all panels.

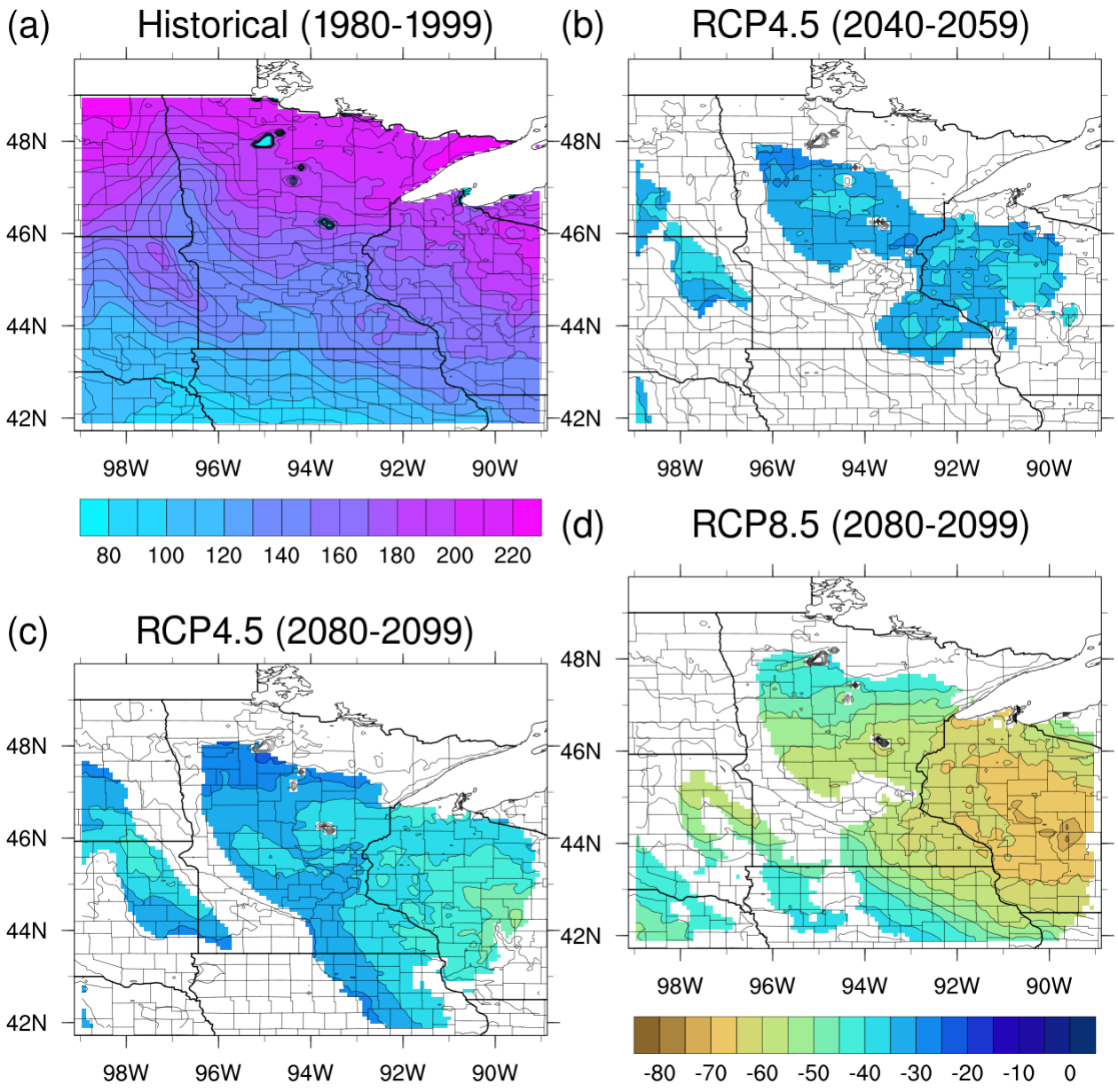

Fig. 8: As Fig. 4, but for MME days per year and difference in days per year with snow height above 0.0254 m (one inch). Please note that there is a different color bar for (a) than for (b-d).